

Atazanavir–bilirubin interaction: a pharmacokinetic–pharmacodynamic model

Roberto Lozano¹
Nieves Domeque²
Alberto-Fermin Apesteguia³

¹Pharmacy Department, ²Psychiatry Department, Hospital Real Nuestra Señora de Gracia, ³Pharmacy Department, Hospital Clínico Universitario “Lozano Blesa”, Zaragoza, Spain

Purpose: The aim of this work was to analyze the atazanavir–bilirubin relationship, using a new mathematical approach to pharmacokinetic–pharmacodynamic models, for competitive drug interactions based on Michaelis–Menten equations.

Patients and methods: Because atazanavir induces an increase of plasma bilirubin levels, in a concentration-dependent manner, we developed a mathematical model, based on increments of atazanavir and bilirubin concentrations at steady state, in HIV infected (HIV⁺) patients, and plotted the corresponding nomogram for detecting suboptimal atazanavir exposure.

Results: By applying the obtained model, the results indicate that an absolute value or an increment of bilirubin at steady state below 3.8 $\mu\text{mol/L}$, are predictive of suboptimal atazanavir exposure and therapeutic failure.

Conclusion: We have successfully implemented a new mathematical approach to pharmacokinetic–pharmacodynamic model for atazanavir–bilirubin interaction. As a result, we found that bilirubin plasma levels constitute a good marker of exposure to atazanavir and of viral suppression.

Keywords: atazanavir, bilirubin, HIV/AIDS, pharmacodynamics, pharmacokinetics

Introduction

Atazanavir ([ATZ] REYATAZ[®]; Bristol-Myers Squibb, New York, NY, USA), an antiretroviral drug belonging to protease inhibitor (PI) class, is widely used to treat infection of human immunodeficiency virus (HIV)/AIDS and to prevent viral replication by selectively binding to viral proteases and blocking proteolytic cleavage of protein precursors. Given the specificity of its target, there is a risk for the development of viral resistance and, consequently, therapeutic failure.¹

The reasons for this therapeutic failure are complex and include the incomplete adherence to therapy and other pharmacokinetic factors. Because of this, therapeutic drug monitoring (TDM) may be used alongside other diagnostic techniques to achieve optimal therapeutic efficacy with minimal toxicity and viral resistance.^{2,3}

Pharmacokinetic differences contribute to variability and frequency of suboptimal antiretroviral exposure.⁴ In this way, TDM can be used to rule out subtherapeutic drug levels resulting from malabsorption, drug interactions, poor adherence, or increased drug metabolism or clearance.⁵ The TDM of protease-inhibitor drugs (PI) includes the study of plasma levels that correlate with clinical failure as one of the most important targets.^{6–8}

Currently, the treatment guidelines for ATZ recommend a minimal effective concentration (MEC) of 0.2 $\mu\text{mol/L}$ for successful viral suppression, and an upper

Correspondence: Roberto Lozano
Pharmacy Service, Hospital Real Nuestra Señora de Gracia, Ramon y Cajal 60, 50004 Zaragoza, Spain
Tel +34 876 764 522
Fax +34 876 764 555
Email rlozano@salud.aragon.es

limit of $<1.1 \mu\text{mol/L}$, because this last recommendation has been associated with a high risk of increased unconjugated bilirubin and incidence of hyperbilirubinemia.^{5,9–11}

We also know that all patients treated with ATZ exhibit a concentration-dependent increase of unconjugated bilirubin and total bilirubin levels (BILs), attributed to a concentration-dependent inhibition of UGT1A1 by ATZ. In contrast, similar direct relationships between ATZ concentrations and virological outcome have not yet been demonstrated.^{12–15}

At this point, a pharmacokinetic–pharmacodynamic (PK–PD) model could be applied to describe the quantitative relationships between the response intensity of a biomarker or surrogate marker (increase in bilirubin plasma levels) and drug dose applied (ATZ plasma levels). This model has two components: a pharmacokinetic model, which will characterize the concentration of ATZ in blood or plasma; and a pharmacodynamic model, which will characterize the pharmacological effect, BIL increase, in this PK–PD drug–interaction based model.^{16,17}

Finally, many authors have suggested that BIL may be used as a marker of adherence to ATZ therapy, exposure, and possible therapeutic outcome.^{9,18,19} However, despite having nomograms for the calculation of exposition to ATZ based on the turnover concept and indirect response model, which support the conventional model in this area,²⁰ the data obtained by applying our present model were not consistent with those obtained by applying nomograms published by other authors.^{9,18–20}

With the above in mind, this work was aimed at developing a new mathematical approach for a competitive–interaction PK–PD model of the ATZ–bilirubin interaction, based on Michaelis–Menten equations, and plotting of the corresponding ATZ–BIL nomogram for predictive detection of ATZ concentrations below MEC and for nonadherence.

Methods

We conducted a retrospective study by reviewing patients treated with ritonavir-boosted ATZ (ATZ-r), to evaluate ATZ-related BIL elevation, as an adherence and exposure marker, for treatments with ATZ.

Patients and sample data

The sample consisted of 47 HIV-infected Hispanic adult outpatients, recruited from the Hospital Clínico Universitario “Lozano Blesa,” Zaragoza, Spain, who were taking antiretroviral therapy (ART), were being managed at a public ART delivery site in Zaragoza, and who had initiated

ART 6–12 months prior to starting the study, which was conducted between September 2011 and April 2012. Patient demographics are shown in Table 1.

The HIV-infected outpatients were taking ATZ-r 300/100 mg, once daily, for at least 6 months, in combination with two nucleoside reverse transcriptase inhibitors (NRTIs) or one NRTI plus one nucleotide reverse transcriptase inhibitor, with combinations that included emtricitabine/tenofovir, lamivudine, tenofovir, and nevirapine, according to the Spanish guidelines for choosing ART (Gesida²¹) (Table 1).

Data of ATZ-r treatments, BILs, viral load (VL), and clinical details were collected from pharmacy dispensing, medical history, and laboratory records.

For the outcome, we chose to look at VL level at four thresholds: VL < 50 copies/mL, VL = 50–1,000 copies/mL, 5,000 $> \text{VL} > 1,000$ copies/mL, and VL $> 5,000$ copies/mL. The last two thresholds were chosen to reflect the World Health Organization (WHO) criteria for prevention of HIV drug resistance ($<1,000$ copies/mL) and treatment failure ($<5,000$ copies/mL) and the first, VL < 50 copies/mL, because pharmacological response correlates very closely with this value.^{22–25}

PK–PD model building

The pharmacokinetics of the ATZ and its BIL response is described by a competitive drug–interaction model, based on Michaelis–Menten kinetics, where hyperbilirubinemia is attributed to a concentration-dependent ATZ inhibition of UGT1A1, the enzyme responsible for bilirubin and ATZ conjugation (Figure 1).

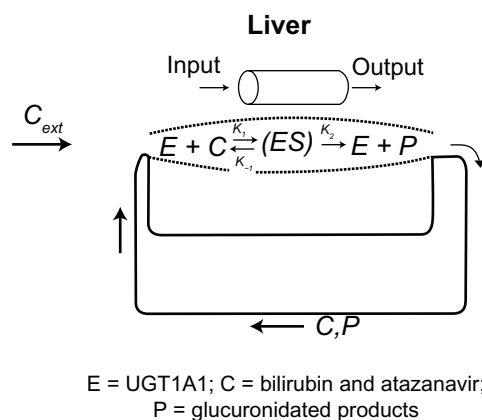
This model describes the influence of two or more drugs acting on the same enzyme and predicts the combined effects of more than one drug, being the analysis of changes

Table 1 Clinical characteristics and antiretroviral-drug status of the patients

	Patient characteristics (n = 47)
Atazanavir-r	100
Women	63
Age (years)	42.1 (8.5)
Weight (kg)	60.7 (13.2)
FTC/TDF	68
NVP	84
3TC	32
TDF	29

Note: All data expressed as mean value (SD), except for Women and antiretroviral-drug percentages.

Abbreviations: TDF, tenofovir; FTC, emtricitabine; 3TC, lamivudine; NVP, nevirapine; SD, standard deviation.



$$V = \frac{d[P]}{dt} = \frac{V_{max} [C]}{K_m + [C]}$$

with

$$K_m = \frac{K_2 + K_{-1}}{K_1} \quad \text{and} \quad V_{max} = K_{cat} E_o$$

Michaelis–Menten equation

Figure 1 Pharmacokinetic–pharmacodynamic (PK–PD) model for bilirubin–atazanavir interaction

Note: Information on the 3 equations taken from.²⁶

in the velocity of reaction that occur when the drugs are used combined versus separately at steady state (SS), the general approach to the study of these interactions.^{12–15,26–28}

Once the SS was reached, we quantified the ATZ–bilirubin interaction by applying the mathematical model, as follows:

Deriving Michaelis–Menten's equation,²⁶

$$V = \frac{K_{cat} E_o C}{K_m + C},$$

for bilirubin and ATZ, we have

$$\frac{dV_{ATZ}}{dC_{ATZ}} = K_{cat}^{ATZ} E_o K_m^{ATZ}$$

and

$$\frac{dV_{BIL}}{dC_{BIL}} = K_{cat}^{BIL} E_o K_m^{BIL}$$

at SS, when

$$dV_{ATZ} = dV_{BIL},$$

then we have

$$\Delta[ATZ]_{ss} = \frac{K_{cat}^{BIL} K_m^{BIL}}{K_{cat}^{ATZ} K_m^{ATZ}} \Delta[BIL]_{ss}$$

and

$$\frac{\Delta[ATZ]_{ss1}}{\Delta[ATZ]_{ss2}} = \frac{\Delta[BIL]_{ss1}}{\Delta[BIL]_{ss2}}, \quad [1]$$

where V = glucuronidation reaction rate for bilirubin and ATZ, respectively; E_o = UGT1A1 enzyme concentration; K_m = Michaelis–Menten constant for bilirubin and ATZ,

respectively; and K_{cat} = turnover number for bilirubin and ATZ, respectively.

Therefore, ATZ and BIL increase plasma levels ($\Delta[ATZ]$ and $\Delta[BIL]$, respectively) of each other in a concentration-dependent manner and allow us to calculate BIL and ATZ increases at SS by using a simple principle of direct proportionality (Equation 1).

Accordingly, $\Delta[BIL]_{ss}$ and $\Delta[ATZ]_{ss}$ values to determinate the risk of underexposure and/or antiviral toxicity can be calculated according to Equation 1 by using bibliographic data for MEC and for the minimal plasmatic concentration at SS (C_{min,ss_ATZ}). Because the latest data (C_{min,ss_ATZ}) are exponential in nature, we used the geometric instead of arithmetic mean for calculations.

The pharmacokinetic characteristics of ATZ are shown in Table 2.

Results

We obtained a mean value for BIL increase at SS ($\Delta[BIL]_{ss}$) equal to 17.1 $\mu\text{mol/L}$, from 10.3 to 28.9 $\mu\text{mol/L}$, related to a theoretical C_{min,ss_ATZ} equal to 0.9 $\mu\text{mol/L}$ ¹ (Table 3).

Substituting into Equation 1 with the following data:

- $\Delta[ATZ]_{ss1} = 0.9 \mu\text{mol/L}$; (as the result of $C_{min,ss_ATZ} = 0.9 \mu\text{mol/L}$ ¹ minus $C_{min,bas_ATZ} = 0 \mu\text{mol/L}$).
- $\Delta[BIL]_{ss1} = 17.1 \mu\text{mol/L}$; (as the result of $BIL_{ss} = 28.9 \mu\text{mol/L}$ minus $BIL_{bas} = 10.3 \mu\text{mol/L}$).
- $\Delta[ATZ]_{ss2} = 0.2 \mu\text{mol/L}$ (MEC of ATZ),

we obtained: $\Delta[BIL]_{ss2} = BIL_{ss} - BIL_{bas} = 3.8 \mu\text{mol/L}$.

Thus, 3.8 $\mu\text{mol/L}$ is the lowest absolute BIL_{ss} value (obtained from $\Delta[BIL]_{ss2} = 3.8$, when $BIL_{bas} = 0$) and the lowest increment of BIL (obtained from $\Delta[BIL]_{ss2} = 3.8$, when $BIL_{bas} \neq 0$), to which C_{min,ss_ATZ} is above 0.2 $\mu\text{mol/L}$ (MEC).

Table 2 Pharmacokinetics data of atazanavir (ATZ) at steady-state (SS)

$C_{\max_SS_ATZ}$ ($\mu\text{mol/L}$)	
Geometric mean (CV %)	6.2 (0.1)
Mean (SD)	7.4 (4.3)
T_{\max} (h)	
Median	3.0
AUC ($\mu\text{mol} \cdot \text{h/L}$)	
Geometric mean (CV %)	65.4 (0.1)
Mean (SD)	76.4 (50.1)
T-half (h)	
Mean (SD)	8.6 (2.3)
$C_{\min_SS_ATZ}$ ($\mu\text{mol/L}$)	
Geometric mean (CV %)	0.9 (0.1)
Mean (SD)	1.2 (1.2)

Note: C_{\max/\min_SS_ATZ} = The maximum/minimum concentration of ATZ at SS.

Abbreviations: AUC, area under the curve; SD, standard deviation; CV, coefficient of variation in %; h, hours.

Accordingly, BIL_{ss} levels can be predicted at the MEC of ATZ ($0.2 \mu\text{mol/L}$) for various BIL_{bas} levels.⁵ In this way, the resulting nomogram was obtained by putting “i” value pairs of BIL_{ss} and BIL_{bas} , in the following equation:

$$\Delta[BIL]_{ss} = [BIL]_{ss\ i} - [BIL]_{bas\ i} = 3.8 \mu\text{mol/L}, \quad [2]$$

where $3.8 \mu\text{mol/L}$ is both the lowest absolute BIL_{ss} value and the lowest increment of BIL, in order to achieve a $C_{\min_SS_ATZ}$ above $0.2 \mu\text{mol/L}$ (MEC) (Figure 2).

On the other hand, and for clinical outcome proposals, we found that 87.2% of patients had $VL < 50$ copies/mL, 6.4% had $VL = 50-1,000$, 0% had $1,000 < VL < 5,000$ copies/mL, and the remaining 6.4% had $VL \geq 5,000$ copies/mL; and regarding BIL_{ss} , 4.4% of patients had $BIL_{ss} < 3.8 \mu\text{mol/L}$, while another 38% had $BIL_{ss} > 30.2 \mu\text{mol/L}$ and high risk of potentially developing toxicity as jaundice eye and/or widespread.

Finally, a patient's likelihood of having $VL \geq 5,000$ copies/mL, the upper limit for absence of viral response according to

Table 3 Results for bilirubin (BIL) plasma levels (up) and viral load (down)

BIL_baseline ($\mu\text{mol/L}$)	BIL_SS ($\mu\text{mol/L}$)		$\Delta [BIL]_{ss} = (BIL_SS) - (BIL_baseline)$ ($\mu\text{mol/L}$)	
10.3 (7.7)	28.9 (21.9)		17.1 (13.1)	
Viral load (copies/mL)	<50	50–1000	1000–5000 (risk viral resistance)	≥ 5000 (risk therapeutic failure)
Patients	87.2	6.4	0	6.4

Notes: All data expressed as mean (SD), except for patients percentage. $BIL_baseline$, is BIL plasma concentration at baseline. BIL_SS , is BIL plasma concentration at steady-state. $\Delta [BIL]_{ss} = (BIL_SS) - (BIL_baseline)$, is BIL plasma concentration increase at steady-state.

Ledergerber et al, associated to $BIL_{ss} \leq 3.8 \mu\text{mol/L}$, was higher than the likelihood associated to $BIL_{ss} > 3.8 \mu\text{mol/L}$ (odds ratio [OR] = 42; 95% CI: 2.6 to 698.6; $P = 0.0086$) (Table 3).²⁹

Discussion

With respect to the model for the quantification of ATZ-bilirubin interaction, previous studies have shown a positive correlation between ATZ exposure and hyperbilirubinemia that allow us to use BIL as a marker of ATZ exposure.^{18–20}

Atazanavir and bilirubin are a substrate for the organic anion-transporting polypeptide (OATP)1B1, p-glycoprotein and UGT1A1, and atazanavir is mainly metabolized by CYP3A4 and UGT1A1. We assumed that induced hyperbilirubinemia by ATZ is due to the inhibition of bilirubin glucuronidation through UGT1A1 enzyme, not taking into consideration the influence from these other transporting and/or metabolizing enzymes, because they do not change the final end point (BIL increase).^{14,15,30–41} Thus, we used BIL_{ss} as surrogate marker in a competitive interaction-based model, where bilirubin elimination through glucuronidation is inhibited by ATZ.

The final BIL_{ss} concentrations are predicted by increments of BIL ($\Delta[BIL]$) plasma levels, from baseline levels to those after ATZ exposure, or by its absolute value, obtained from $\Delta[BIL]$ when $BIL_{bas} = 0$. In any case, the final BIL_{ss} are in direct dependence of the ATZ, being desirable to achieve a minimal BIL_{ss} concentration above $3.8 \mu\text{mol/L}$ for the proposed ATZ $> 0.2 \mu\text{mol/L}$.⁵

The present model is based on the study of the increments of ATZ and BIL, as model components, once the SS is reached. Thus, because this model is only dependent on concentration increments of interacting drugs (from drug concentration at the start of the interaction to drug concentration at SS) and is not a kinetic model, where the concentration is expressed as a function of time, the present model is only applicable once SS is reached, as for an adherence marker. Also, our model is independent of the pharmacokinetic model used, whereas the models based on the turnover concept, where a drug can inhibit or stimulate the production or elimination of a given variable, by contrast, are linked to a pharmacokinetic model and are applicable at any time with the plasma concentration of the drug as a function of time.^{19,20}

This turnover system is described with differential equations, where dR/dt is a function of K_{in} and K_{out} with R = response. In the drug induced inhibition models (I_{max}

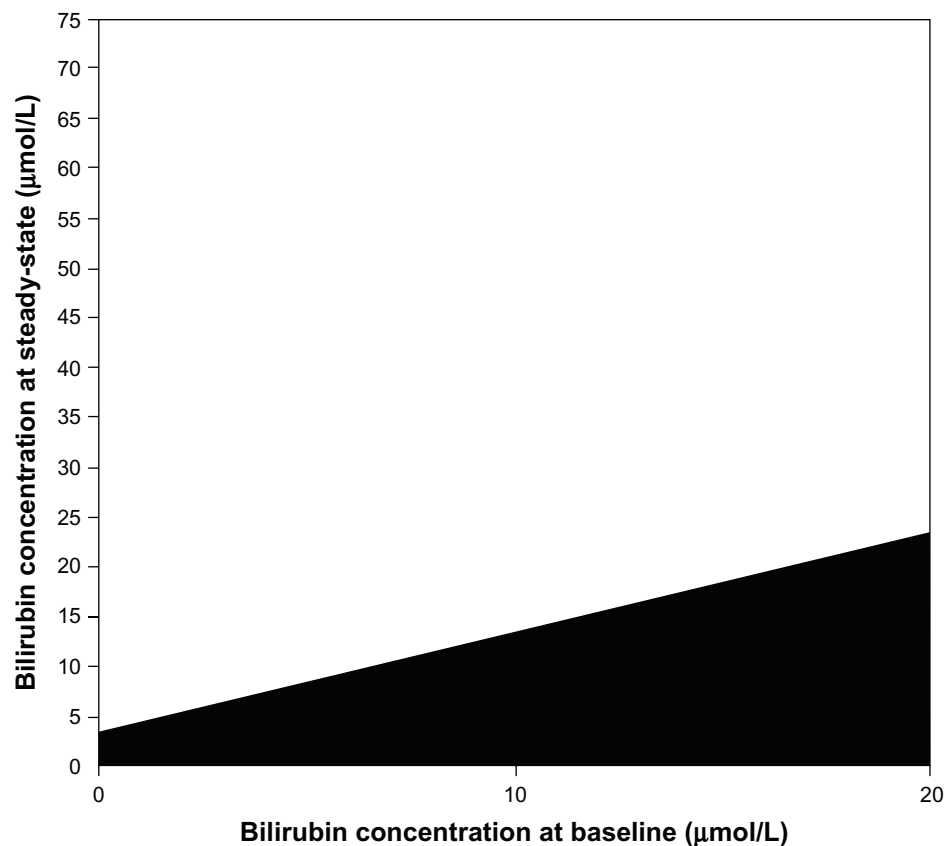


Figure 2 The black area represents bilirubin steady state levels (BILss) associated with atazanavir (ATZ) exposure below minimal effective concentration (MEC), 0.2 $\mu\text{mol/L}$; and white area represents BILss associated with ATZ concentrations over MEC.

models), with impact on the output (K_{out}), as for the conventional model in this interaction, we have:

$$\frac{dR_{\text{BIL}}}{dt} = K_{\text{in}} - k_{\text{out}} \left[1 - \left(\frac{I_{\text{max}} C_{\text{ATZ}}}{C_{\text{ATZ}} + \text{IC50}_{\text{ATZ}}} \right) \right] R_{\text{BIL}} \quad [3]$$

where

$$H(C) = I(C) \text{ def} = \left[1 - \left(\frac{I_{\text{max}} C_{\text{ATZ}}}{C_{\text{ATZ}} + \text{IC50}_{\text{ATZ}}} \right) \right]. \quad [4]$$

Here, “def = ” means that the quantity on the left is defined to the quantity on the right. The action of the drug takes place on $H(C)$, where $C = C(t)$ is the plasma concentration of the drug as a function of time (the drug function), taking place, in the case of ATZ–bilirubin interaction, via the loss term K_{out} , because ATZ inhibits and reduces the bilirubin elimination (response). In addition, these nonlinear models need previous estimates of K_{in} (production rate of pharmacological response), I_{max} (maximal drug induced inhibition), IC50 (concentration at 50 percent of maximal drug induced inhibition) or, alternatively, to be viewed as

linear function, as follows: $I(C) = 1 - \alpha C$, when $C \ll \text{IC50}$, and the parameter α determined from the slope of the graph of AUC-R(D) versus $\log(D)$.^{42–44}

Consequently, indirect response models have to establish a priori bounds on the response function ($R[t]$), on the peak time (T_{max}), and on the area under the curve (AUC-R).

Regarding the nomogram, as a result of applying the equations of our exposed mathematical model, based on changes of the reaction velocity of ATZ versus that of BIL, with the implicated enzyme UGT1A1, we obtained a relation of simple proportionality for the increments of ATZ and BIL plasma concentrations at SS (Equation 1), which we used to obtain the nomogram, illustrating the mentioned proportionality between BIL_{bas} and BIL_{ss} of patients on treatment with the same dose of ATZ. BIL_{ss} data placed on the white area of the nomogram indicate an ATZ exposure over MEC ($>0.2 \mu\text{mol/L}$), while on the black area this means an ATZ exposure below MEC ($<0.2 \mu\text{mol/L}$). The minimal value of BIL_{ss} for exposition to optimal ATZ concentration is $3.8 \mu\text{mol/L}$.

In the nomogram, BIL_{ss} values and its corresponding BIL_{bas} values are associated and, in order to predict an ATZ concentration above 0.2 (MEC), two separate measurements of bilirubin are needed (at baseline and at SS), except in the case of $BIL_{ss} < 3.8$ (minimal absolute value), where this one value alone is enough. At this point, the conventional model cannot provide the threshold minimum value data and, also, the areas corresponding to suboptimal exposure to ATZ do not match ours.²⁰

The second part of this work has been motivated by the potential benefits of BIL_{ss} as a measure of long-term adherence or exposure regarding virological outcomes. Given that ATZ increases BIL_{ss} in an exposure-dependent manner, we tested whether BIL_{ss} levels could be used as a surrogate marker of virological response to ATZ-based ART regimens.

Previous studies have shown a positive correlation between atazanavir exposure and hyperbilirubinemia but only, in some cases, hyperbilirubinemia have been correlated to virological failure.^{9,30} In this way, we have studied this relation between plasma concentrations of bilirubin and virological failure ($VL \geq 5,000$ copies/mL after 6 weeks of ART), having found an increased risk of virological failure in patients treated with ATZ and who had $BIL_{ss} < 3.8 \mu\text{mol/L}$ ($OR = 42$). Thus, BIL_{ss} would be a practical marker of long-term ATZ exposure.

In short, the great majority of adherent patients treated with standard doses of ATZ-r have drug concentrations above MEC; however, our results support the routine use of atazanavir TDM, based on BIL_{ss} , for efficacy optimization of the treatments and for avoiding adverse events and drug interactions with the use of these drugs.

Nevertheless more studies with larger number of patients with therapeutic failure are necessary, to achieve a better verification of the correlation between BIL_{ss} and VL.

Conclusion

The nomogram and mathematical model discussed in this paper allow us to calculate the patient exposure to ATZ plasma levels above $0.2 \mu\text{mol/L}$ and to assess the patient risk of virological failure based on data of BIL at SS and at baseline, in a quick and easy way.

We can also conclude that there is a minimum BIL at SS, equal to $3.8 \mu\text{mol/L}$, whatever the mathematical model used and different from zero, below which ATZ does not reach a minimal effective concentration; consequently, the risk of virological failure increases.

Thus, bilirubin constitutes a good marker of long-term exposure to ATZ and virological failure for patients being treated with this drug.

Disclosure

The authors report no conflicts of interest in this work.

References

1. REYATAZ® (atazanavir sulfate) [package insert]. *Highlights of Prescribing Information*. Princeton, NJ; Bristol-Meyers Squibb; 2013. Available from: http://packageinserts.bms.com/pi/pi_reyataz.pdf. Accessed August 10, 2013.
2. Fraaij PL, Rakhmanina N, Burger DM, de Groot R. Therapeutic drug monitoring in children with HIV/AIDS. *Ther Drug Monit*. 2004;26(2):122–126.
3. Rakhmanina NY, van den Anker JN, Soldin SJ, van Schaik RH, Mordwinkin N, Neely MN. Can therapeutic drug monitoring improve pharmacotherapy of HIV infection in adolescents? *Ther Drug Monit*. 2010;32(3):273–281.
4. Kearns GL, Abdel-Rahman SM, Alander SW, Blowey DL, Leeder JS, Kauffman RE. Developmental pharmacology – drug disposition, action, and therapy in infants and children. *N Engl J Med*. 2003;349(12):1157–1167.
5. Panel on Antiretroviral Guidelines for Adults and Adolescents. *Guidelines for the Use of Antiretroviral Agents in HIV-1-Infected Adults and Adolescents*. Department of Health and Human Services; 2013. Available from: <http://www.aidsinfo.nih.gov/ContentFiles/AdultandAdolescentGL.pdf>. Accessed August 10, 2013.
6. Acosta EP, Gerber JG; Adult Pharmacology Committee of the AIDS Clinical Trials Group. Position paper on therapeutic drug monitoring of antiretroviral agents. *AIDS Res Hum Retroviruses*. 2002;18(12): 825–834.
7. Anderson PL, Fletcher CV. Updated clinical pharmacologic considerations for HIV-1 protease inhibitors. *Curr HIV/AIDS Rep*. 2004;1(1): 33–39.
8. Morse GD, Catanzaro LM, Acosta EP. Clinical pharmacodynamics of HIV-1 protease inhibitors: use of inhibitory quotients to optimise pharmacotherapy. *Lancet Infect Dis*. 2006;6(4):215–225.
9. Josephson F, Andersson M, Flamholz L, et al. The relation between treatment outcome and efavirenz, atazanavir or lopinavir exposure in the NORTHIV trial of treatment-naïve HIV-1 infected patients. *Eur J Clin Pharmacol*. 2010;66(4):349–357.
10. la Porte CJL, Back DJ, Blaschke T, et al. Updated guideline to perform therapeutic drug monitoring for antiretroviral agents. *Reviews in Antiviral Therapy*. 2006;3:4–14.
11. Colombo S, Buclin T, Cavassini M, et al. Population pharmacokinetics of atazanavir in patients with human immunodeficiency virus infection. *Antimicrob Agents Chemother*. 2006;50:3801–3808.
12. Lozano R, Marin R, Pascual A, Santacruz MJ, Lozano A, Sebastian F. Biomarkers and therapeutic drug monitoring in psychiatry. In: *Biomarker*. Khan TK, editor. Rijeka, Croatia: InTech; 2012. Available from: <http://www.intechopen.com/books/biomarker/biomarkers-and-therapeutic-drug-monitoring-in-psychiatry>. Accessed August 10, 2013.
13. Zhang D, Chando T, Everett D, Patten C, Dehal S, Humphreys W. In vitro inhibition of UDP glucuronosyltransferases by atazanavir and other HIV protease inhibitors and the relationship of this property to in vivo bilirubin glucuronidation. *Drug Metab Dispos*. 2005;33(11):1729–1739.
14. Smith D, Jeganathan S, Ray J. Atazanavir plasma concentrations vary significantly between patients and correlate with increased serum bilirubin concentrations. *HIV Clinical Trials*. 2006;7(1):34–38.
15. Cleijnsen RM, van de Ende ME, Kroon FP, et al. Therapeutic drug monitoring of the HIV protease inhibitor atazanavir in clinical practice. *J Antimicrob Chemother*. 2007;60(4):897–900.
16. Breimer DD, Danhof M. Relevance of the application of pharmacokinetic-pharmacodynamic modelling concepts in drug development. The “wooden shoe” paradigm. *Clin Pharmacokinet*. 1997;32:259–267.
17. Geldof M, Freijer J, van Beijsterveldt L, Danhof M. Pharmacokinetic modeling of non-linear brain distribution of fluvoxamine in the rat. *Pharm Res*. 2008;25(4):792–804.

18. Petersen K, Riddle M, Jones L, et al. Use of bilirubin as a marker of adherence to atazanavir-based antiretroviral therapy. *AIDS*. 2005; 19(15):1700–1702.
19. Jusko WJ, Ko HC. Physiologic indirect response models characterize diverse types of pharmacodynamic effects. *Clin Pharmacol Ther*. 1994;56(4):406–419.
20. Rekić D, Clewe O, Røshamar D, et al. Bilirubin-a potential marker of drug exposure in atazanavir-based antiretroviral therapy. *AAPS J*. 2011;13(4):598–605.
21. Panel de expertos de Gesida y Plan Nacional sobre el Sida. [Consensus document of Gesida and Spanish Secretariat for the National Plan on AIDS (SPNS) regarding combined antiretroviral treatment in adults infected by the human immunodeficiency virus (Jan 2012)]. *Enferm Infecc Microbiol Clin*. 2012;30(6):e1–e89. Spanish [with English abstract].
22. Jordan MR, Bennett DE, Bertagnolio S, Gilks CF, Sutherland D. World Health Organization surveys to monitor HIV drug resistance prevention and associated factors in sentinel antiretroviral treatment sites. *Antivir Ther*. 2008;13 Suppl 2:15–23.
23. *Antiretroviral therapy for HIV Infection in Adults and Adolescents. Recommendations for a Public Health Approach*. Geneva: World Health Organization; 2010. Available from: http://whqlibdoc.who.int/publications/2010/9789241599764_eng.pdf. Accessed August 10, 2013.
24. Siliciano RF. Scientific rationale for antiretroviral therapy in 2005: viral reservoirs and resistance evolution. *Top HIV Med*. 2005;13(3):96–100.
25. Nettles RE, Kieffer TL, Simmons RP, et al. Genotypic resistance in HIV-1-infected patients with persistently detectable low-level viremia while receiving highly active antiretroviral therapy. *Clin Infect Dis*. 2004;39(7):1030–1037.
26. Michaelis L, Menten ML, Johnson KA, Goody RS. The original Michaelis constant: translation of the 1913 Michaelis-Menten paper. *Biochemistry*. 2011;50:8264–8269.
27. Dailly E, Tribut O, Tattevin P, et al. Influence of tenofovir, nevirapine and efavirenz on ritonavir-boosted atazanavir pharmacokinetics in HIV-infected patients. *Eur J Clin Pharmacol*. 2006;62:523–526.
28. Solas C, Gagnieu MC, Ravoux I, et al. Population pharmacokinetics of atazanavir in human immunodeficiency virus-infected patients. *Ther Drug Monit*. 2008;30:670–673.
29. Ledergerber B, Lundgren JD, Walker AS, et al; PLATO Collaboration. Predictors of trend in CD4-positive T-cell count and mortality among HIV-1-infected individuals with virological failure to all three antiretroviral-drug classes. *Lancet*. 2004;364(9428):51–62.
30. Karlström O, Josephson F, Sönnernborg A. Early virologic rebound in a pilot trial of ritonavir-boosted atazanavir as maintenance monotherapy. *J Acquir Immune Defic Syndr*. 2007;44(4):417.
31. Morello JE, Cuenca L, Vispo E. Use of serum bilirubin levels as surrogate marker of early virological response to atazanavir-based antiretroviral therapy. *AIDS Res Hum Retroviruses*. 2011;27(00):2–5.
32. Annaert P, Ye Z, Stieger B, Augustijns P. Interaction of HIV protease inhibitors with OATP1B1, 1B3, and 2B1. *Xenobiotica*. 2010;40(3):163–176.
33. Cui Y, König J, Leier I, Buchholz U, Keppler D. Hepatic uptake of bilirubin and its conjugates by the human organic anion transporter SLC21A6. *J Biol Chem*. 2001;276(13):9626–9630.
34. Mediavilla M, Pascolo L, Rodríguez J, Guibert E, Ostrow J, Tiribelli C. Uptake of [(3)H]bilirubin in freshly isolated rat hepatocytes: role of free bilirubin concentration. *FEBS Lett*. 1999;463(1–2):143–145.
35. Hartkoorn R, Kwan W, Shallcross V, et al. HIV protease inhibitors are substrates for OATP1A2, OATP1B1 and OATP1B3 and lopinavir plasma concentrations are influenced by SLCO1B1 polymorphisms. *Pharmacogenet Genomics*. 2010;20(2):112–120.
36. Campbell S, Morais S, Xu J. Inhibition of human organic anion transporting polypeptide OATP1B1 as a mechanism of drug-induced hyperbilirubinemia. *Chem Biol Interact*. 2004;150(2):179–187.
37. Perloff ES, Duan SX, Skolnik PR, Greenblatt DJ, von Moltke LL. Atazanavir: effects on P-glycoprotein transport and CYP3A metabolism in vitro. *Drug Metab Dispos*. 2005;33(6):764–770.
38. Busti AJ, Hall RG, Margolis DM. Atazanavir for the treatment of human immunodeficiency virus infection. *Pharmacotherapy*. 2004;24(12):1732–1747.
39. Rodríguez-Nóvoa S, Martín-Carbonero L, Barreiro P, et al. Genetic factors influencing atazanavir plasma concentrations and the risk of severe hyperbilirubinemia. *AIDS*. 2007;21(1):41–46.
40. Rodríguez Nóvoa S, Barreiro P, Rendón A, et al. Plasma levels of atazanavir and the risk of hyperbilirubinemia are predicted by the 3435C-->T polymorphism at the multidrug resistance gene 1. *Clin Infect Dis*. 2006;42(2):291–295.
41. Monaghan G, Ryan M, Hume R, Burchell B, Seddon R. Genetic variation in bilirubin UDP-glucuronosyltransferase gene promoter and Gilbert's syndrome. *Lancet*. 1996;347(9001):578–581.
42. Peletier LA, Gabrielsson J, Haag Jd. A dynamical systems analysis of the indirect response model with special emphasis on time to peak response. *J Pharmacokinet Pharmacodyn*. 2005;32(3–4):607–654.
43. Ekblad EB, Licko V. A model eliciting transient responses. *Am J Physiol*. 1984;246(1 Pt 2):R114–R121.
44. Dayneka NL, Garg V, Jusko WJ. Comparison of four basic models of indirect pharmacodynamic responses. *J Pharmacokinet Biopharm*. 1993;21:457–478.

Clinical Pharmacology: Advances and Applications

Publish your work in this journal

Clinical Pharmacology: Advances and Applications is an international, peer-reviewed, open access journal publishing original research, reports, reviews and commentaries on all areas of drug experience in humans. The manuscript management system is completely online and includes a very quick and fair peer-review system, which is all easy to use.

Submit your manuscript here: <http://www.dovepress.com/clinical-pharmacology-advances-and-applications-journal>

Dovepress

Visit <http://www.dovepress.com/testimonials.php> to read real quotes from published authors.